



25<sup>th</sup> ABCM International Congress of Mechanical Engineering  
October 20-25, 2019, Uberlândia, MG, Brazil

## COBEM2019-1605

# NUMERICAL SIMULATION OF THE FLOW AROUND A 2D TRIANGULAR RIDGE USING OPENFOAM<sup>®</sup>

**Arthur Leite Guilherme**

**Gilberto Augusto Amado Moreira**

Universidade Federal da Paraíba, Cidade Universitária - João Pessoa - PB - Brasil - CEP: 58051-970.

arthur.guilherme@cear.ufpb.br

gilberto@cear.ufpb.br

**Giuliano Gardolinski Venson**

Universidade Federal de Uberlândia, , Centro de Ciências Exatas e Tecnologia, Faculdade de Engenharia Mecânica.

venson@ufu.br

**Abstract.** *Turbulence can be described as fluctuations in the field of flow in space and time. The process of forming and developing a turbulence is complex, since it is three-dimensional, transient and has several scales. In addition, it can cause significant effects on flow characteristics. When the forces of inertia of the fluid become significant, if compared with the viscous forces, it occurs to the turbulence and it presents in a high number of Reynolds. In this work, the RANS-based turbulence models used in OpenFOAM (Open Field Operation and Manipulation) were tested in unstructured hybrid meshes and their results compared to experimental data performed in a triangular 2D elevation. The results showed, even if simulated in a two-dimensional condition, good agreement with the experimental ones and a good computational performance, compared with the results obtained numerically with Ansys CFX<sup>TM</sup> commercial code.*

**Keywords:** *Computer Fluid Dynamics, OpenFOAM, Open Source, Turbulence Models.*

## 1. INTRODUCTION

The understanding of the wind flow in the atmospheric boundary layer (ABL) on real topographies is of interest in several areas, such as meteorology, environment, architecture, energy production, among others. A good understanding of their behavior results, for example, in the proper positioning of wind turbines; in a good contribution to the analysis and optimization of the dispersion of pollutants in open mines and in the improvement of the constructive aspects of a vertical structure (Blocken *et al.*, 2007; Azad, 1993; Flores *et al.*, 2014).

Numerical simulation is the best, perhaps the only, way to obtain the flow field in a detailed way, especially in large systems, taking into account also the phenomenon of turbulence, present in almost all flows in nature. Therefore, CFD (Computational Fluid Dynamics) analysis is widely used for these purposes (Versteeg and Malalasekera, 2007). The RANS technique (Reynolds Averaged Navier Stokes), which makes use of the temporal mean of the governing equations (Navier-Stokes equations), is the most adequate for the analysis of the ABL, due to its low computational cost relative to other methods, as can be seen in the literature.

The high cost of software licenses commonly used in industry prohibits, or limits, their use for research and small-scale projects. Released under the GNU General Public License, OpenFOAM (Open Source Field Operation and Manipulation) open-source software appears as the solution to this problem. In light of this, this paper tests the RANS-based turbulence models of OpenFOAM software using unstructured hybrid meshes and compares their results with experimental data. The air recirculation size and velocity profiles at a 2D elevation in triangular form, obtained by Arya and Shipman (1981), are used as experimental parameters for comparison with the results of the models.

When dealing with a turbulent flow, and therefore with unpredictable and small-scale fluctuations, Reynolds proposed the decomposition of the instantaneous flow variables into mean value components and floating components. The replacement of these components in the Navier-Stokes equations and the application of the temporal average results in the RANS (Reynolds Averaging Navier Stokes). Such equations will be reported in the next section.

At this point, there are several models of theories and correlations with the purpose of calculating the turbulent viscosity. The four main categories are: zero equation models, one equation models, two equations models, and second order closure models.

In this article we test some turbulence models of two equations for the atmospheric boundary layer flow on a 2D elevation in the extreme situation of a triangular ridge. Here the size of the recirculation and velocity profiles after the ridge is analyzed. The OpenFOAM library was used in this investigation.

In Juretić and Kozmar (2013) used wind tunnel geometry with von Neumann boundary conditions applied at the

inlet and the outlet boundaries to obtain homogeneous mean velocity, turbulent kinetic energy and Reynolds shear stress profiles with various RANS turbulence models, which obtained interesting results and reported difficulties in modeling near the wall due to the shear stress approximation and the experimental results.

The standard  $k-\epsilon$  model, established by Launder and Sharma (1974), is one of the most common turbulence models, despite being imprecise under conditions of large adverse pressure gradients (Wilcox, 2006). Three other models derived from this are: the model proposed by Hargreaves and Wright (2007), here referred as modified  $k-\epsilon$ , which has a modified constant; the  $k-\epsilon$  realizable model (Liou *et al.*, 1995) and the RNG  $k-\epsilon$  model (Yakhot *et al.*, 1992). Other models of two equations are based on the turbulence specific dissipation rate  $\omega$ , these are  $k-\omega$  model (Wilcox, 2006) and the  $k\Omega$  SST model, implemented in OpenFOAM as a variant of the SST  $k-\omega$  model of Menter *et al.* (2003), beyond the SSG Reynolds Stress turbulence model, proposed by Speziale *et al.* (1991).

## 2. PHYSICAL PROBLEM AND MODEL DESCRIPTION

### 2.1 Physical problem

In general, the evaluation of the turbulence model applied here, which will later be applied to a type of atmospheric circulation, may comprise two main processes that dominate its evolution: a) Mechanical effects caused by the topographic or structural obstacles with which the flow interacts, leading to acceleration or recirculation zones. b) Buoyancy effects caused by the heat flux from or towards the surface, which can generate important vertical air flow accelerations. These convective effects depend on the stability of the atmosphere, so that stratification must be taken into account. Both processes interact with each other and are directly influenced by the intense turbulence that characterizes many environmental flows. However, we focus only on the Mechanic to reproduce Arya and Shipman (1981) work, but to apply in GLA it is necessary to implement the thrust that interacts with the mechanic and can influence the turbulent scales.

### 2.2 Solver - OpenFOAM library

The OpenFOAM is a collection of C++ libraries designed to solve complex problems in fluid mechanics. Developed with the desire of obtaining a more effective numerical platform than Fortran, it has benefitted from the new C++ object-oriented programming functionality. Its completely free distribution and the flexibility it offers allow the development of specific solvers by the user, which can be integrated with already existing tools. As most of the CFD codes currently used in engineering, it uses a finite volume formulation. Within its libraries, OpenFOAM integrates turbulence models (RANS and LES), thermophysical models, radiation models and wall functions, which can be accessed when developing a solver. Furthermore, the code offers the functions of integrating complex geometries in the calculation, through the use of the snappyHexMesh tool. For an extensive review of the numerical methods used by the code, as well as of the available tools, we refer to the available documentation OpenCFD (2016)

There are several examples of the application of OpenFOAM to the study of atmospheric flows. Garcia and Boulanger (2006) simulated the wind flow over Mount Saint Helens in the United States employing OpenFOAM with a standard  $k-\epsilon$  RANS turbulence model. A similar work was done by Hussein and El-Shishiny (2009) studying the wind flow over the Giza Plateau in Egypt. Larsson *et al.* (2009) used OpenFOAM to model the non-buoyant wind flow over complex terrain using RANS turbulence models with wall functions, to make accurate predictions of wind power production. Churchfield (2010) developed an OpenFOAM solver using LES to simulate buoyant flows under the Boussinesq approximation, focusing on the flow interaction with wind turbines. Flores *et al.* (2014) used a DES (Detached Eddy Simulation) approach implemented in OpenFOAM to understand the buoyant effect in pollutant dispersion in Chuquicamata, a large open pit mine in Chile. Our interest is to study the problem using an approach to evaluate turbulence and complex geometry in order to analyze a real topography in the future, even without the explicit basis of density variables, the treatment of stratification and buoyancy consequences in the future. be applied to other models, but our goal is to compare the same model applied in Ansys CFX™ compared to OpenFOAM.

#### 2.2.1 Governing equations and implementation in OpenFOAM

OpenFOAM uses the finite volume method for numerical representation of the equations governing fluid motion and the message passing interface (MPI) method for parallel computing. The toolbox features a range of numerical schemes, methods and turbulence models. The available turbulence models range from Reynolds averaged Navier–Stokes (RANS) to hybrid RANS/LES (HRL) to LES. It is also possible to resolve all scales using direct numerical simulation (DNS). The governing equations for incompressible fluid flow are the Navier–Stokes equations:

$$\nabla \cdot \vec{U} = 0 \quad (1)$$

$$\frac{\partial \vec{U}}{\partial t} + (\vec{U} \cdot \nabla) \vec{U} = \nabla \cdot \left\{ (\nu + \nu_t) (\nabla \vec{U} + \nabla \vec{U}^t) \right\} \quad (2)$$

where  $U$  is the fluid velocity vector,  $p$  is the density-normalized pressure,  $\nu$  is the kinematic viscosity of the fluid, and  $\nu_t$  is the turbulent viscosity of the fluid. OpenFOAM provides three different pressure–velocity coupling methods for solving these equations: PISO (pressure implicit with split operator) (Issa, 1986); SIMPLE (semi-implicit method for pressure linked equations) (Patankar and Spalding, 1972); and PIMPLE, which is a hybrid of PISO and SIMPLE. The SIMPLEC (SIMPLE consistent) algorithm is also available, but only as part of the pressure based compressible solver rhoSimplecFoam. Since much detailed information is available in (Jasak, 1996), the following provides only a summary of the salient aspects of the incompressible numerical methods and models.

Boussinesq (1877) hypothesized that the Reynolds tensor is a linear function of the mean velocity gradient, for incompressible flows, with eddy viscosity  $\mu_t$  being analogous to the dynamic viscosity in the shear stress equation. Equation (1) defines the eddy viscosity as the product between density, a characteristic length scale of turbulence ( $l$ ) and velocity  $V_t$ .

$$\mu_t = \rho \cdot V_t \cdot l \quad (3)$$

Where  $V_t$ , in most models is given by the root of turbulent kinetic energy ( $k$ ) (Moukalled *et al.*, 2016).

### 2.2.2 Incompressible PISO/PIMPLE/SIMPLE solvers

The governing equations are generally solved using standard pressure–velocity coupling methodology- (1) momentum predictor,(2) pressure solver, (3) momentum corrector. The PIMPLE algorithms a unique variation of the PISO method, where an outer correction loops, i.e., cycling over a given time step for a number of iterations, and equation under-relaxation between outer correctors are allowed for stability. If no outer corrector loops are used, the algorithm is directly equivalent to the PISO method. PIMPLE solver also includes dynamic time-stepping (automatic time step adjustment to maintain a certain CFL number). The simpleFoam solver is based on the SIMPLE algorithm. It pursues a steady-state solution with the aid of under-relaxation factors between iterations. Equation under-relaxation helps promote diagonal dominance by boosting the influence of the owner cell terms (Jasak, 1996).

Given the need to incorporate stratification into the model, we use a quasi-compressible approximation, including density as an explicit variable in the calculation. A detailed view of the algorithms used in OpenFOAM to couple pressure and velocity in the compressible case (PISO type algorithms, Pressure-Implicit with Splitting of Operators), can be found in (Paulo J. Oliveira, 2001).

The great advantage of OpenFOAM is that each one of the above terms can easily be incorporated or eliminated from the solver that is used for each simulation, given that each application can be compiled independently. In summary, the solver includes the following equations: continuity, momentum conservation (Navier–Stokes), enthalpy conservation, ideal gas state and passive scalar transport, using the libraries and tools provided by OpenFOAM to solve them (thermo-physical, turbulence and finite volume libraries). For Arya and Shipman (1981) work this study uses the model based on the SIMPLE algorithm, which in OpenFOAM is simpleFOAM.

### 2.2.3 Finite volume discretization

Integral over a conjectural control volume  $V_p$  for a general scalartransport equation leads to:

$$\left[ \underbrace{\frac{\partial}{\partial t} \int_{V_p} \phi dV}_{time} + \underbrace{\int_{V_p} \nabla \cdot (\vec{U} \phi) dV}_{divergence} - \underbrace{\int_{V_p} \nabla \cdot (\Gamma \nabla \phi) dV}_{Laplacian} \right] = SOURCE \quad (4)$$

A comprehensive list of the numerical methods available in OpenFOAM can be found in (Robertson *et al.*, 2015). The following provides some details of selected discretization methods used in the study.

### 2.2.4 Geometry and meshing

Given our interest in working with complex geometries, we use the GMSH tool, although OpenFOAM offers the snappyHexMesh alternative OpenCFD (2010) to solve the mesh generation problem. GMSH has proven to be very versatile when applied to different domain configurations. In particular, it allows STL files to be used as precursors for mesh generation, enabling the inclusion of complex geometric shapes and even topography in simulations. In most cases we use GMSH itself which is free software, despite the flexibility of working with files from other software such as STL format. The meshes consisted of hexahedra (hex) and split-hexahedra (split-hex) cells. In cases with complex geometry the mesh was refined near the walls to produce cells with wall normal dimensions between  $y_1^+ = 10$  and  $y_1^+ = 300$  adjacent to the surface. However, it is impossible to satisfy this criteria everywhere when processes of flow separation and attachment occur.

### 2.2.5 Treatment of walls

OpenFOAM offers a series of specialized libraries to define the boundary conditions on a surface. It has been shown Tominaga *et al.* (2008) that in the case of complex configurations that include a set of buildings or obstacles, it is preferable to use a smooth wall condition, given that a rough wall model requires a large grid, which makes it difficult to capture the details of the flow in complex geometries. Although different works have shown rough walls to be crucial in maintaining the correct ABL profiles along the upwind fetch, in this work any effect of the surface roughness is assumed to be small compared with the effects of the terrain, as suggested in (Silvester *et al.*, 2009). There are many considerations to take into account when using wall functions in RANS simulations, considering the advantages and limitations of each wall model. For an extensive review, see (Blocken *et al.*, 2007). However the results shown in this work correspond to Low Re wall function using URANS simulations to compare results.

### 2.2.6 Initial and boundary conditions

In CFD the initial and boundary conditions used are of fundamental importance, because they directly affect the evolution of the simulation and must necessarily take into account the physical processes that we are modelling. Although OpenFOAM offers a wide variety of pre-defined conditions, in the majority of case, it is necessary to create specific conditions for each simulation. Furthermore, there exist important differences whether the simulation considers buoyant effects or not.

There are different alternatives to define the inlet velocity profile, depending on the information available. If we have experimental data, we can use the expression:

$$U(z) = \frac{u_*}{\kappa} \ln\left(\frac{z+z_0}{z_0}\right) \quad (5)$$

where  $u_*$  (friction velocity) and  $z_0$  (roughness height) are known or can be estimated from data and  $\kappa$  is a constant with approximate value of 0.4.

Richards and Hoxey (1993) proposed inlet boundary conditions consistent the k- $\epsilon$  model defined by Eq. 5 for stream-wise velocity and Equations 6 and 7 for turbulent kinetic energy and dissipation rate of turbulent energy, respectively:

$$k = \frac{u_*^2}{\sqrt{C_\mu}} \quad (6)$$

$$\epsilon = \frac{u_*^3}{\kappa(z+z_0)} \quad (7)$$

where  $C_\mu$  is a model constant. In URANS simulations these profile is maintained fixed as a forcing during the entire simulation. The outlet profile of velocity is defined as zero gradient, assuming a fully developed flow.

The top boundary condition is normally set as zero gradient due to its practicality, however it is inconsistent with inlet Richard and Hoxey conditions, except under certain circumstances (O'Sullivan *et al.*, 2011). A constant shear stress should be applied as the domain is sufficiently small to be entirely inside the constant shear stress layer. As reported in O'Sullivan *et al.* (2011) work this condition return the von Neumann conditions as the following equations:

$$\frac{\partial U}{\partial z} = \frac{u_*}{\kappa(z+z_0)} \quad (8)$$

$$\frac{\partial \epsilon}{\partial z} = \frac{-u_*^3}{\kappa(z+z_0)^2} \quad (9)$$

Already the lateral contour condition was used an empty condition, which is suggested by (OpenCFD, 2016) for two-dimensional simulations.

### 2.2.7 Turbulence models

The turbulence models compared in this study are separated into two groups. The first is based on turbulent viscosity models, which contains the standard k- $\epsilon$ , k- $\epsilon$  realizable and RNG k- $\epsilon$  model. Besides these, there are more two models based on the turbulence specific dissipation rate  $\omega$ , these are k- $\omega$  model and another model implemented in OpenFOAM as a variant of the SST k- $\omega$  model of Menter *et al.* (2003). The second group used is based on Reynolds stress modeling, where only one model was used in this work, the SSG Reynolds Stresses.

For the k- $\epsilon$ , RNG k- $\epsilon$ , k- $\omega$  and SST k- $\omega$  models, the results are also compared with those obtained numerically by Martins *et al.* (2003).

The standard  $k-\epsilon$  model is one of the most prominent turbulence models and has therefore been implemented in CFD for many different purposes as it is considered the industry standard model. It has been proven to be stable and numerically well constituted. In addition, it has a well-established prediction capacity regime. For general simulations, this model offers a good yield in terms of approximation and constitution. However, there are some applications for which this model is not indicated, which may include: boundary layer separation flows; flows with sudden changes in choke rates; flow in rotating fluids; flow on curved surfaces. The RNG  $k-\epsilon$  model is an alternative to the standard  $k-\epsilon$  model. In general, it offers a better improvement over the boundary layer recirculation size compared to the standard  $k-\epsilon$  model.

The Realizable  $k-\epsilon$ , developed by (Shih *et al.*, 1995), differs from the standard  $k-\epsilon$  model in two ways. Firstly it contains a new formulation for the turbulent viscosity:  $C\mu$  is not a constant like in the standard model but a variable. The second difference is a new transport equation for the dissipation rate, that is derived from an exact equation for the transport of the mean-square vorticity fluctuation. As a result it mainly gives improved predictions for superior ability to capture the mean flow of complex structures and for flows involving rotation, boundary layers under strong adverse pressure gradients, separation and re circulation.

The  $k-\omega$  model is an alternative for predicting Low Reynolds number flows, whereas the SST model has a blend function that applies in regions near the wall the  $k-\omega$  model and in regions where there are recirculations away from the wall, the standard  $k-\epsilon$  model.

Finally, the SSG Reynolds Stress model, proposed by Speziale *et al.* (1991), was chosen because it did not have to modify the meshes used in this study, being possible to keep the same configuration for all models. These model use the exact Reynolds stress transport equation for their formulation. They account for the directional effects of the Reynolds stresses and the complex interactions in turbulent flows. Reynolds stress models offer significantly better accuracy than eddy-viscosity based turbulence models, while being computationally cheaper than DNS and LES methods.

### 3. METODOLOGY

Numerical tests using the recirculation size and velocity profiles obtained experimentally by Arya and Shipman (1981) were performed with different turbulence models.

The experimental results of Arya and Shipman (1981) were obtained in a wind tunnel with a section 1.8m wide, 1.5m high and 11m long, where the intensity and size of the turbulence scales were controlled for a neutral atmospheric boundary layer. The uncertainty regarding the results obtained was 15 %. The geometric parameters of the triangular surface have height  $H = 0.15\text{m}$  and width of base  $B = 0.385\text{m}$ , as shown in Figure 1.

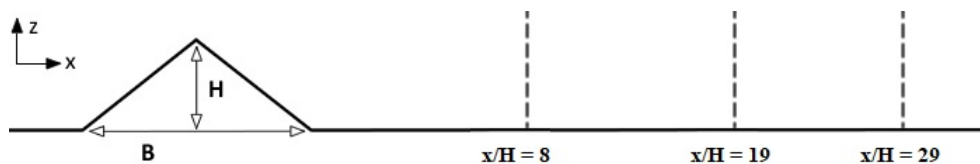


Figure 1. Out-of-scale graphical representation of the triangular surface with the locations of the experimental velocity profiles.

To obtain the experimental data, Arya and Shipman (1981) subjected the wind tunnel to a free stream velocity of 8 m/s. The developed boundary layer reached the height of 1.5 m near the ridge, so these reference values, together with the roughness height  $z_0$  of 0.25 mm, were imposed on inlet through Eq. (5). The coordinate system has been changed to be a function of the height of the triangular surface ( $H$ ). The origin,  $x = 0$ , was chosen to be the triangle base. As a result, a recirculation size of  $13H$  was found and explored for the velocity path at positions  $x/H = 8$ ,  $x/H = 19$  and  $x/H = 29$ .

For the definition of the mesh, several mesh tests were performed with the standard  $k-\epsilon$  model to define which mesh presented parameters close to those considered ideal by OpenCFD (2010) and eventual convergence with this model. The best mesh for this model was identified, this was applied to the other models of turbulence, already mentioned previously. The models that did not converge with the mesh used in the standard  $k-\epsilon$  model, due to differences in the distance from the first node to the wall, were treated separately, performing other mesh tests for these models.

The solver used was simpleFoam based on the SIMPLE algorithm, in addition to using the boundary conditions provided for atmospheric flow. The simulations were performed on a Dell PowerEdge server and met the  $10^{-5}$  error criteria for the velocity field and  $10^{-4}$  for the other quantities.

### 4. RESULTS

Table 1 shows the results obtained from the literature and the results of the turbulence models tested. The first line presents the experimental results obtained by Arya and Shipman (1981). In the second and third line are presented the numerical results obtained by Moreira *et al.* (2010) for the  $k-\epsilon$  models and the RNG $k-\epsilon$  model. The subsequent lines of the table present the numerical results of the OpenFoam.

The recirculation size with the RNG  $k-\epsilon$  and SST  $k-\omega$  and SSG models is within the Arya and Shipman experimental error margin of 15%. Possible sources of error for the numerical results are the fact that there is an extreme condition of pointed obstacle that causes unorthogonality in cells near the summit (Moukalled *et al.*, 2016; Mouzakis and Bergels, 1991), necessary for  $y_+$  configuration; the aspect ratio, that is, the difference between adjacent cell volumes near the summit and the fact that it was simulated in a 2D domain, which does not take into account a three-dimensional nature of turbulence.

Table 1. Recirculation size after triangular structure.

Turbulence Model / Experimental Measurement	Recirculation Size
Experimental Arya and Shipman (1981)	13.0 H
$k-\epsilon$ Moreira <i>et al.</i> (2010)	8.7 H
RNG $k-\epsilon$ Moreira <i>et al.</i> (2010)	13.1 H
$k-\omega$ Moreira <i>et al.</i> (2010)	6.7 H
SST $k-\omega$ Moreira <i>et al.</i> (2010)	9.3 H
SSG <sup>1</sup> Moreira <i>et al.</i> (2010)	20.3 H
$k-\epsilon^1$	8.60 H
Modified $k-\epsilon^1$	8.40 H
Realizable $k-\epsilon^1$	11.47 H
RNG $k-\epsilon^1$	12.53 H
$k-\omega^1$	9.93 H
SST $k-\omega^1$	13.00 H
SSG <sup>1</sup>	13.01 H

(1) Present study

The results obtained for the models  $k-\epsilon$  and RNG  $k-\epsilon$  were inferior to those obtained numerically by Martins *et al.* (2003), but present differences smaller than 15%. The standard  $k-\epsilon$  model presented results far from the experimental values of Arya and Shipman (1981), with differences of 33%, as also shown by Martins *et al.* (2003).

Although it has a more robust implementation accounting Reynolds tensor anisotropy, the SSG model does not give very accurate results for near-wall velocity. Therefore, it has shown ability to predict recirculation size, as seen in Tab. 1, what was very more effective in this work rather than in Moreira *et al.* (2010) work, possibly due to either the applied top conditions or the used softwares.

For the profile at  $x/H = 8$  the numerical results are very close to the experimental measurements from  $z = 1.8H$ . In experimental measurements below  $z = 0.5H$ , as pointed out by Mouzakis and Bergels (1991) and Kim and Patel (2000), there is an inconsistency with the fact that this profile “cuts” the recirculation zone, where it is expected negative values, being attributed to this inability the instruments used to detect direction.

For the profiles at  $x/H = 19$  and  $x/H = 29$  (Fig. 2b and Fig. 3), the  $k-\omega$ ,  $k-\epsilon$  and modified  $k-\epsilon$  models performed in this work showed good agreement with the experimental results, where they have average errors less than 5%. However, they assumed the worst recirculation size values, with an error of 25% for the  $k-\omega$  model. This fact is due to the ability of this model to act near walls and the inability to predict recirculation size. Even so, it presents an error about 50% smaller than the same model implemented with Ansys CFX in Moreira *et al.* (2010) work.

The SST  $k-\omega$  model, together with the SSG model, also yields interesting results, but the combined need for a much more refined mesh and the resulting increased computational cost makes it less appropriate than the RNG  $k-\epsilon$  and realizable  $k-\epsilon$  for this case.

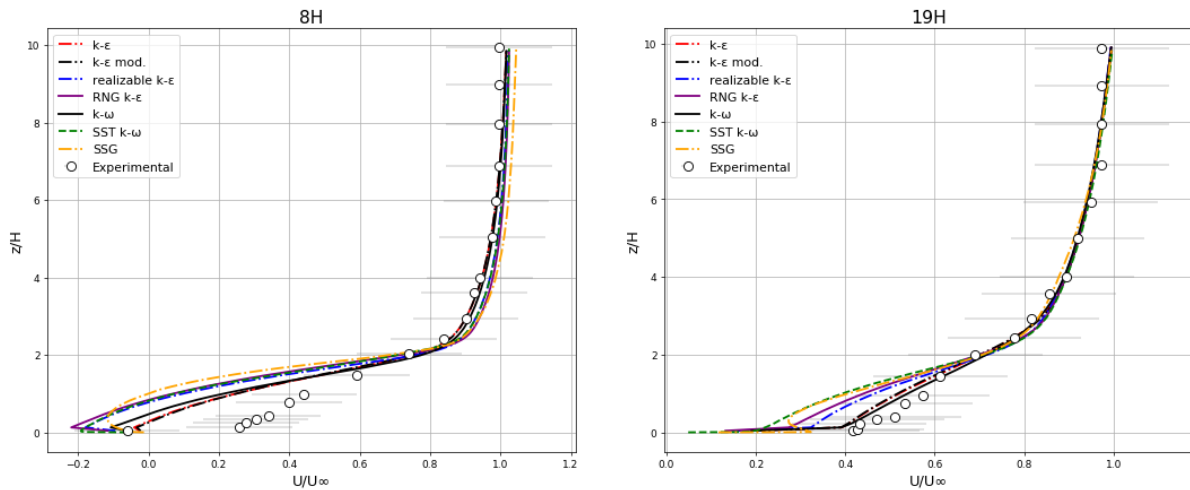


Figure 2. Velocity profile at (a)  $x/H = 8$  and (b)  $x/H = 19$

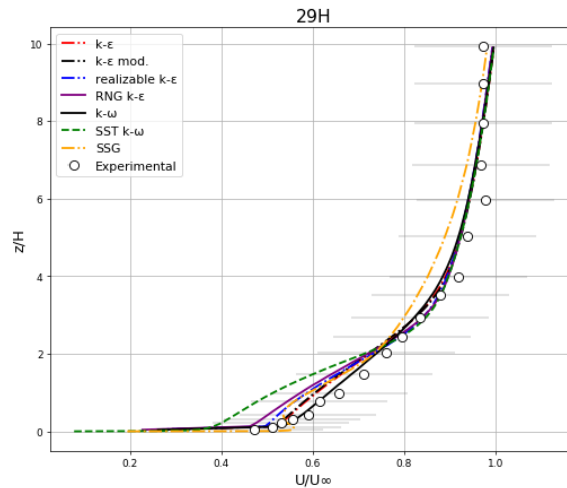


Figure 3. Velocity profile at  $x/H = 19$ .

## 5. CONCLUSIONS

The applied boundary conditions from Richard present in this work showed to be consistent when applied to the numerical model replicated in this work. Here, the method found to be the most appropriate is the RNG  $k-\epsilon$ , strengthening this qualitative result also found by Kim and Patel (2000), denote the full capacity of the OpenFOAM library to develop low cost CFD analysis. Reynolds stress models have good robustness, but required more computational power and according to the literature, their application would become more viable if the model were 3D. The model is not relatively new and optimizing additional models can improve model prediction for non-neutral stratifications, but its relatively simple, free application may be a good option ahead of commercial solutions. Future work involving complex real terrain geometries will be studied with this software, which will be based on the choice of turbulence models present here.

## 6. ACKNOWLEDGEMENTS

The authors thank the CNPQ for the resources and the maintenance of the scholarship to the student.

## 7. REFERENCES

- Arya, S. and Shipman, M., 1981. "An experimental investigation of flow and diffusion in the disturbed boundary layer over a ridge—i. mean flow and turbulence structure". *Atmospheric Environment (1967)*, Vol. 15, No. 7, pp. 1173 – 1184. ISSN 0004-6981. doi:[https://doi.org/10.1016/0004-6981\(81\)90308-5](https://doi.org/10.1016/0004-6981(81)90308-5). URL <http://www.sciencedirect.com/science/article/pii/0004698181903085>.
- Azad, R.S., 1993. *The atmospheric boundary layer for engineers*, Vol. 17. Springer Science & Business Media.

- Blocken, B., Stathopoulos, T. and Carmeliet, J., 2007. "Cfd simulation of the atmospheric boundary layer: wall function problems". *Atmospheric Environment*, Vol. 41, No. 2, pp. 238 – 252. ISSN 1352-2310. doi:<https://doi.org/10.1016/j.atmosenv.2006.08.019>. URL <http://www.sciencedirect.com/science/article/pii/S135223100600834X>.
- Boussinesq, J., 1877. "Essai sur la theorie des eaux courantes". *Mem. Acad. Sci. Inst. Fr.*, Vol. 23, No. 1, pp. 252–260.
- Churchfield, M., 2010. "A description of the openfoam solver buoyantboussinesqpisifoam, national renewable energy laboratory, national wind technology centre".
- Flores, F., Garreaud, R. and Muñoz, R.C., 2014. "Openfoam applied to the cfd simulation of turbulent buoyant atmospheric flows and pollutant dispersion inside large open pit mines under intense insolation". *Computers & Fluids*, Vol. 90, pp. 72–87.
- Garcia, M. and Boulanger, P., 2006. "Low altitude wind simulation over mount saint helens using nasa srtm digital terrain model". *Third International Symposium on 3D Data Processing, Visualization, and Transmission (3DPVT'06)*, pp. 535–542.
- Hargreaves, D. and Wright, N., 2007. "On the use of the k–e model in commercial cfd software to model the neutral atmospheric boundary layer". *Journal of Wind Engineering and Industrial Aerodynamics*, Vol. 95, pp. 355–369. doi:10.1016/j.jweia.2006.08.002.
- Hussein, A.S. and El-Shishiny, H., 2009. "Influences of wind flow over heritage sites: A case study of the wind environment over the giza plateau in egypt". *Environ. Model. Softw.*, Vol. 24, No. 3, pp. 389–410. ISSN 1364-8152. doi:10.1016/j.envsoft.2008.08.002. URL <http://dx.doi.org/10.1016/j.envsoft.2008.08.002>.
- Issa, R., 1986. "Solution of the implicitly discretised fluid flow equations by operator-splitting". *Journal of Computational Physics*, Vol. 62, No. 1, pp. 40 – 65. ISSN 0021-9991. doi:[https://doi.org/10.1016/0021-9991\(86\)90099-9](https://doi.org/10.1016/0021-9991(86)90099-9). URL <http://www.sciencedirect.com/science/article/pii/0021999186900999>.
- Jasak, H., 1996. *Error analysis and estimation for finite volume method with applicationsto fluid flows*. Ph.D. thesis, Imperial College, University of London.
- Juretić, F. and Kozmar, H., 2013. "Computational modeling of the neutrally stratified atmospheric boundary layer flow using the standard k– turbulence model". *Journal of Wind Engineering and Industrial Aerodynamics*, Vol. 115, pp. 112 – 120. ISSN 0167-6105. doi:<https://doi.org/10.1016/j.jweia.2013.01.011>. URL <http://www.sciencedirect.com/science/article/pii/S0167610513000378>.
- Kim, H.G. and Patel, V., 2000. "Test of turbulence models for wind flow over terrain with separation and recirculation". *Boundary-Layer Meteorology*, Vol. 94, pp. 5–21. doi:10.1023/A:1002450414410.
- Larsson, E.U., Cehlin, S.M., Openfoam, U. and Tapia, X.P., 2009. "Environment modelling of wind flow over complex terrain".
- Launder, B. and Sharma, B., 1974. "Application of the energy-dissipation model of turbulence to the calculation of flow near a spinning disc". *Letters in Heat and Mass Transfer*, Vol. 1, No. 2, pp. 131 – 137. ISSN 0094-4548. doi:[https://doi.org/10.1016/0094-4548\(74\)90150-7](https://doi.org/10.1016/0094-4548(74)90150-7). URL <http://www.sciencedirect.com/science/article/pii/0094454874901507>.
- Liou, T.H.S.W.W., Shabbir, A., Yang, Z. and Zhu, J., 1995. "A new k-e eddy viscosity model for high reynolds number turbulent flows". *Computers and Fluids*, Vol. 24, pp. 227–238.
- Martins, M.A., Valle, R.M. and França, G.A.C., 2003. "Test of turbulence models for wind flow on the downwind slope of a 2d ridge model in neutral atmosphere." *17th International Congress of Mechanical Engineering*.
- Menter, F., Kuntz, M. and Langtry, R., 2003. "Ten years of industrial experience with the sst turbulence model". *Heat and Mass Transfer*, Vol. 4.
- Moreira, G.A.A., Valle, R.M., Martins, M.A. and Nascimento, C.A.M., 2010. "Estudo teórico do escoamento turbulento sobre terrenos complexos para uma região de belo horizonte." *Io Seminário Nacional Sobre Engenharia do Vento - SENEV 2010, Belo Horizonte*.
- Moukalled, F., Mangani, L. and Darwish, M., 2016. *The Finite Volume Method in Computational Fluid Dynamics*. Springer International Publishing, Switzerland, 1st edition.
- Mouzakis, F.N. and Bergels, G.C., 1991. "Numerical prediction of turbulent flow over a two-dimensional ridge". *International Journal for Numerical Methods in Fluids*, Vol. 12, No. 3, pp. 287–296. doi:10.1002/flf.1650120306. URL <https://onlinelibrary.wiley.com/doi/abs/10.1002/flf.1650120306>.
- OpenCFD, 2010. "Openfoam advanced training." OpenFOAM Version 1.7.
- OpenCFD, 2016. "User and programmer's guide." OpenFOAM Version 1.6.
- O'Sullivan, J., Archer, R. and Flay, R., 2011. "Consistent boundary conditions for flows within the atmospheric boundary layer". *Journal of Wind Engineering and Industrial Aerodynamics*, Vol. 99, No. 1, pp. 65 – 77. ISSN 0167-6105. doi:<https://doi.org/10.1016/j.jweia.2010.10.009>. URL <http://www.sciencedirect.com/science/article/pii/S0167610510001182>.
- Patankar, S. and Spalding, D., 1972. "A calculation procedure for heat, mass and momentum transfer in three-dimensional parabolic flows". *International Journal of Heat and Mass Transfer*, Vol. 15,

- No. 10, pp. 1787 – 1806. ISSN 0017-9310. doi:[https://doi.org/10.1016/0017-9310\(72\)90054-3](https://doi.org/10.1016/0017-9310(72)90054-3). URL <http://www.sciencedirect.com/science/article/pii/S0017931072900543>.
- Paulo J. Oliveira, R.I.I., 2001. “An improved piso algorithm for the computation of buoyancy-driven flows”. *Numerical Heat Transfer, Part B: Fundamentals*, Vol. 40, No. 6, pp. 473–493. doi:[10.1080/104077901753306601](https://doi.org/10.1080/104077901753306601). URL <https://doi.org/10.1080/104077901753306601>.
- Richards, P. and Hoxey, R., 1993. “Appropriate boundary conditions for computational wind engineering models using the k- turbulence model”. *Journal of Wind Engineering and Industrial Aerodynamics*, Vol. 46-47, pp. 145 – 153. ISSN 0167-6105. doi:[https://doi.org/10.1016/0167-6105\(93\)90124-7](https://doi.org/10.1016/0167-6105(93)90124-7). URL <http://www.sciencedirect.com/science/article/pii/S0167610593901247>. Proceedings of the 1st International on Computational Wind Engineering.
- Robertson, E., Choudhury, V., Bhushan, S. and Walters, D., 2015. “Validation of openfoam numerical methods and turbulence models for incompressible bluff body flows”. *Computers and Fluids*, Vol. 123, pp. 122–145.
- Shih, T.H., Liou, W.W., Shabbir, A., Yang, Z. and Zhu, J., 1995. “A new k- eddy viscosity model for high reynolds number turbulent flows”. *Computers Fluids*, Vol. 24, No. 3, pp. 227 – 238. ISSN 0045-7930. doi:[https://doi.org/10.1016/0045-7930\(94\)00032-T](https://doi.org/10.1016/0045-7930(94)00032-T). URL <http://www.sciencedirect.com/science/article/pii/S004579309400032T>.
- Silvester, S., Lowndes, I. and Hargreaves, D., 2009. “A computational study of particulate emissions from an open pit quarry under neutral atmospheric conditions”. *Atmospheric Environment*, Vol. 43, No. 40, pp. 6415 – 6424. ISSN 1352-2310. doi:<https://doi.org/10.1016/j.atmosenv.2009.07.006>. URL <http://www.sciencedirect.com/science/article/pii/S1352231009005858>.
- Speziale, C.G., Sarkar, S. and Gatski, T.B., 1991. “Modelling the pressure–strain correlation of turbulence: an invariant dynamical systems approach”. *Journal of Fluid Mechanics*, Vol. 227, p. 245–272. doi:[10.1017/S0022112091000101](https://doi.org/10.1017/S0022112091000101).
- Tominaga, Y., Mochida, A., Yoshie, R., Kataoka, H., Nozu, T., Yoshikawa, M. and Shirasawa, T., 2008. “Aij guidelines for practical applications of cfd to pedestrian wind environment around buildings”. *Journal of Wind Engineering and Industrial Aerodynamics*, Vol. 96, No. 10, pp. 1749 – 1761. ISSN 0167-6105. doi:<https://doi.org/10.1016/j.jweia.2008.02.058>. URL <http://www.sciencedirect.com/science/article/pii/S0167610508000445>. 4th International Symposium on Computational Wind Engineering (CWE2006).
- Versteeg, H.K. and Malalasekera, W., 2007. *An introduction to computational fluid dynamics: the finite volume method*. Pearson education.
- Wilcox, D.C., 2006. *Turbulence Modeling for CFD*. DCW Industries, Inc., Canada., 3rd edition.
- Yakhot, V., Orszag, S.A., Thangam, S., Gatski, T.B. and Speziale, C.G., 1992. “Development of turbulence models for shear flows by a double expansion technique”. *Physics of Fluids A: Fluid Dynamics*, Vol. 4, No. 7, pp. 1510–1520. doi:[10.1063/1.858424](https://doi.org/10.1063/1.858424). URL <https://doi.org/10.1063/1.858424>.

## 8. RESPONSIBILITY NOTICE

The authors are the only responsible for the printed material included in this paper.